CHAPTER IV
RESULTS AND DISCUSSION

In the previous study (Wongpraphairoat, 2013), the dehydroxylation of glycerol to propylene glycol was investigated over copper/zinc oxide-based catalysts prepared by incipient wetness impregnation over various supports—i.e. aluminum oxide (Al_2O_3), amorphous silica-alumina (ASA), magnesium oxide (MgO), and hydrotalcite ($Mg_6Al_2CO_3(OH)_{16}\cdot 4(H_2O)$). The result showed that $CuZnO/Al_2O_3$ gave the highest catalytic activity followed by CuZnO/MgO, CuZnO/HT, CuZnO/ASA, respectively. This could be due to the largest surface area of $CuZnO/Al_2O_3$. Noticeably, CuZnO/MgO exhibited the highest stability when alkali (Na, K) contaminated feed was used. Therefore, the present study focused on catalysts prepared by co-precipitation method with an intention to improve the catalytic activity and maintain the stability of CuZnO/MgO catalyst.

4.1 Catalytic Characterization

Table 4.1 provides the textual properties of MgO support, CuZnO/MgO catalysts. After impregnated and co-precipitated of the catalyst, it is clearly seen that decreases in surface area and pore volume were observed when compared to the MgO support. This might be due to the high amount of metal loading that could plug the pore of the support. Although the surface area of CuZnO/MgO catalyst prepared by impregnation is higher than that prepared by co-precipitation this probably due to the lower amount of MgO support in co-precipitated catalyst, observed by AAS as shown in Table 4.2.

Table 4.1 BET surface area, pore volume, and pore size distribution of the support and the catalysts

Catalysts	Surface area (m^2/g)	Pore volume (cm^3/g)	Pore diameter (nm)
MgO support	168.00	0.360	1.028
CuZnO/MgO (IWI)	21.16	0.195	1.027
CuZnO/MgO (COP)	4.33	0.068	1.028
CuZnO (COP)	3.11	0.058	1.129

* calculated using BJH method

Atomic absorption spectroscopy (AAS) was employed to examine the actual metal loading of the Cu, Zn, and Mg deposited on the catalysts. The AAS results are summarized in Table 4.2. The result indicated that the amounts of Cu and Zn remained invariant compared to the expected metal loading in catalyst prepared by incipient wetness impregnation. Whereas the amount of Cu and Zn in catalyst prepared by co-precipitation was higher than that expected because Mg was not efficiently precipitated in the catalyst. This is probably due to pH value at 10.5 in the catalyst preparation, since Mg easily precipitated in acidic aqueous solution, as reported by Yamamoto *et al.* (2006). These results described the very low amount of Mg was precipitated, this affected the co-precipitated catalyst to have lower surface area and pore volume than the impregnated catalyst. Comparing between two types of co-precipitated catalysts, The CuZnO has lower catalyst surface area than the CuZnO/MgO. This result indicated that the incorporated MgO could be perform the higher catalyst surface area and affected the Cu better dispersed.

Table 4.2 The actual and expected metal loading of the catalysts

CuZnO/MgO	**Cu (wt.%)**	**Zn (wt.%)**	**MgO (wt.%)**
Expected loading	10.00	41.38	48.82
Actual loading (IWI)	9.55	38.75	43.82
Actual loading (COP)	12.85	49.97	21.32

Figure 4.1 shows the XRD patterns of the CuZnO/MgO catalysts prepared by different methods after calcined at 550 °C for 6 h. The XRD patterns of the impregnated and co-precipitated catalysts were quite similar, consisting of ZnO phase which appeared at 2-theta of 31.7°, 34.4°, 36.2°, 47.6, 56.5°, 62.9°, 66.3°, 67.9° and 69.0°. The CuO phase appeared at 2-theta of 35.4°, 38.8° and 48.6°.The peak of CuO in the co-precipitated catalyst exhibited bigger than that of impregnated catalyst due to the higher amount of Cu in the co-precipitated catalyst. Nevertheless, MgO phase was found in the impregnated catalyst at 2-theta of 42.8° and 62.1° and no reflection line assigned to Mg species in the co-precipitated catalyst. This is probably due to a very low content of MgO since Mg was not sufficiently deposited in the catalyst during co-precipitation.

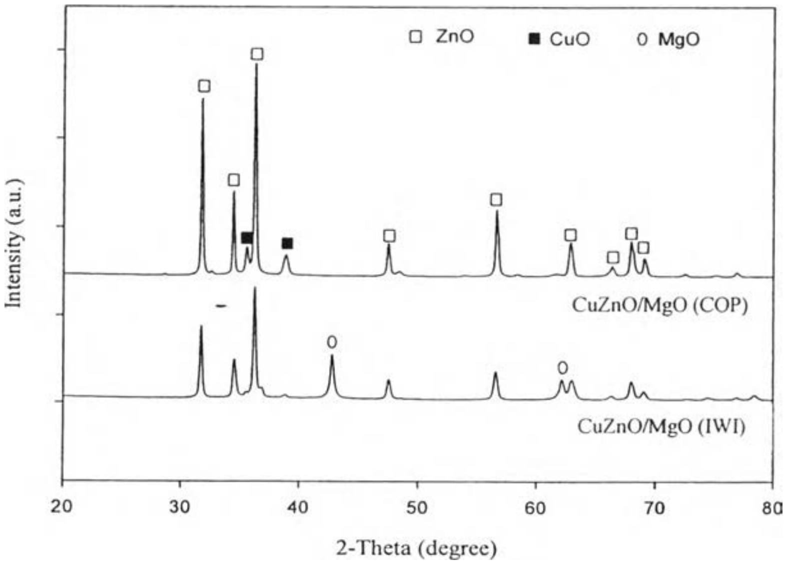

Figure 4.1 XRD patterns of the fresh CuZnO/MgO catalysts with different preparation methods.

In order to determine the reduction behavior of the catalysts, H_2–TPR studies were carried out in the temperature range from room temperature to 800 °C. The TRR profiles of the fresh catalysts are shown in Figure 4.2. The co-precipitated catalysts showed two regions of reduction peak, the first region attributed to a reduction peak of CuO (Cu^{2+}) and the second region represented a reduction peak of Cu_2O (Cu^{1+}). However, the reduction peak of the CuZnO (COP) shift to higher reduction temperatures as well as a pronounced broadening of the reduction peak indicates large and less dispersed copper particles (Kurr *et al.*, 2008). In case of the CuZnO/MgO (IWI) catalyst, a single peak was observed between 200 °C and 450 °C which broader peak compared to the reduction peak of the co-precipitated catalysts. In this case, the H_2 consumption is much less than the co-precipitated catalyst indicating that the lower in CuO species was reduced. This result is in good agreement with the earlier study (Panyad *et al.*, 2011).

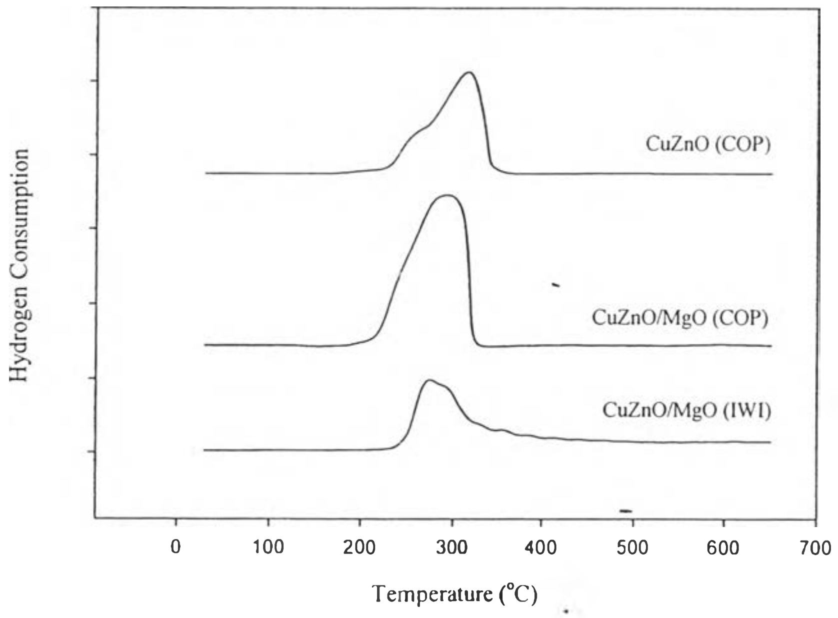

Figure 4.2 Temperature programmed reduction (TPR) profiles of the fresh CuZnO/MgO catalysts with different preparation methods.

4.2 Catalytic Activity Testing

4.2.1 Effect of Catalyst Preparation

In this study, the activities of catalysts prepared by different procedures for incipient wetness impregnation and co-precipitation are compared as shown in Figure 4.3. The experimental results demonstrated that the catalytic activity of the CuZnO/MgO (COP) catalyst was higher than that of CuZnO/MgO (IWI) catalyst. However, the CuZnO (COP) showed lower catalytic activity than the CuZnO/MgO (COP) catalyst. This result indicated that the mixing of Cu and Zn could be performed the reaction, whereas Mg could act like a promoter in case of co-precipitation.

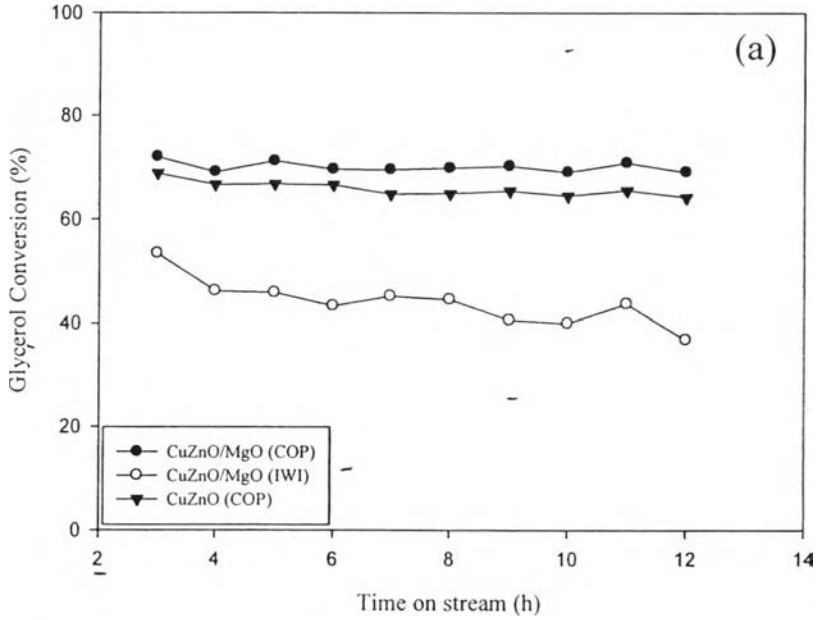

Figure 4.3 Plots of (a) Glycerol Conversion and (b) PG Selectivity (c) Acetol Selectivity (d) EG Selectivity as a function of time on stream over the CuZnO/MgO catalysts prepared by different methods. (Reaction conditions: 80 wt.% glycerol feed, 250 °C, 500 psig, H_2:glycerol = 4:1, and WHSV = 3.77 h^{-1}).

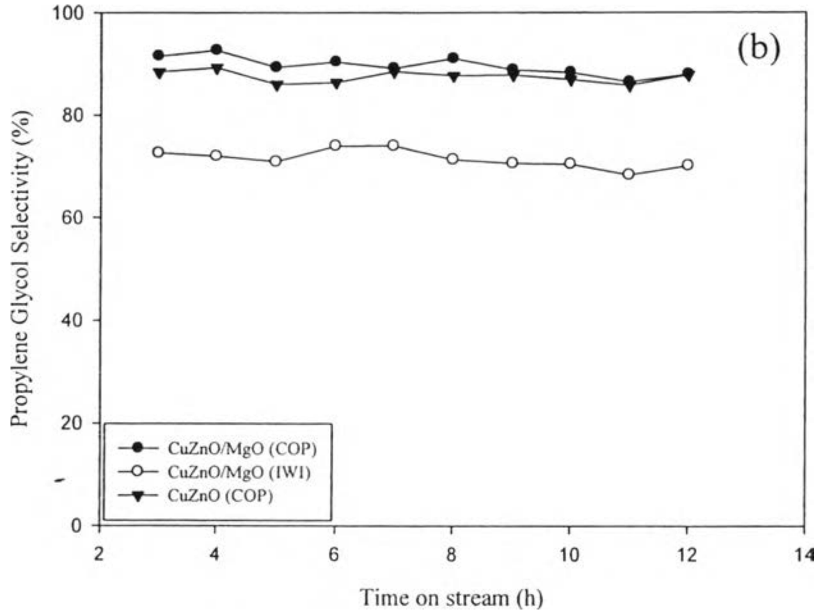

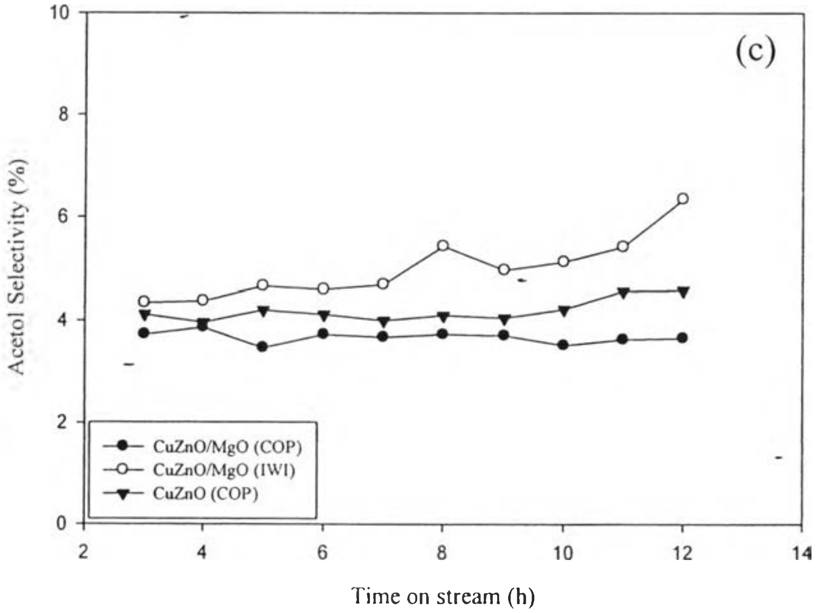

Figure 4.3 (cont.) Plots of (a) Glycerol Conversion and (b) PG Selectivity (c) Acetol Selectivity (d) EG Selectivity as a function of time on stream over the CuZnO/MgO catalysts prepared by different methods. (Reaction conditions: 80 wt.% glycerol feed, 250 °C, 500 psig, H_2:glycerol = 4:1, and WHSV = 3.77 h^{-1}).

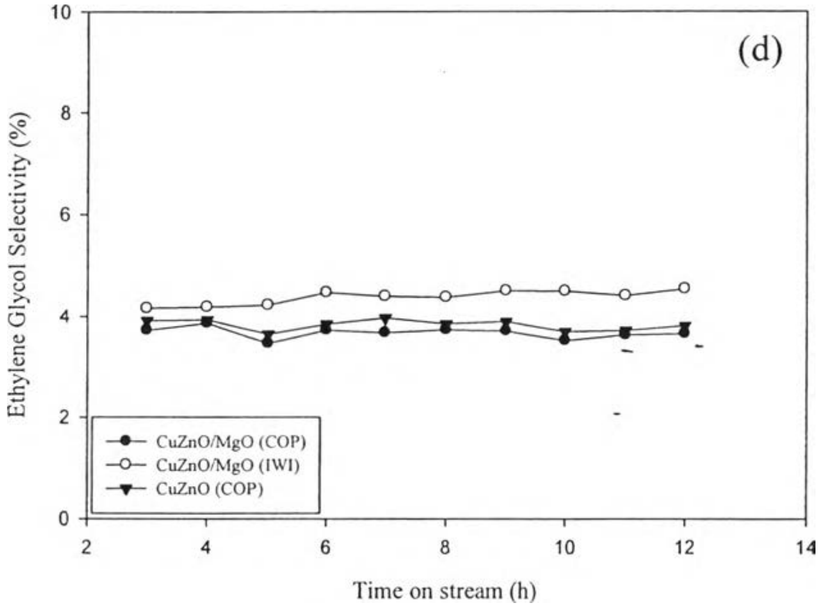

Figure 4.3 (cont.) Plots of (a) Glycerol Conversion and (b) PG Selectivity (c) Acetol Selectivity (d) EG Selectivity as a function of time on stream over the CuZnO/MgO catalysts prepared by different methods. (Reaction conditions: 80 wt.% glycerol feed, 250 °C, 500 psig, H_2:glycerol = 4:1, and WHSV = 3.77 h^{-1}).

From Figures 4.3 (b) and (c), the decreased of propylene glycol selectivity led to the increased of acetol selectivity. The results well agreed with the mechanism proposed by Dasari *et al.* (2005), as shown in Figure 4.4. Moreover, another by-product like ethylene glycol was observed. This may be formed by another reaction route, as proposed by Feng *et al.* (2008) (Fig.2.11).

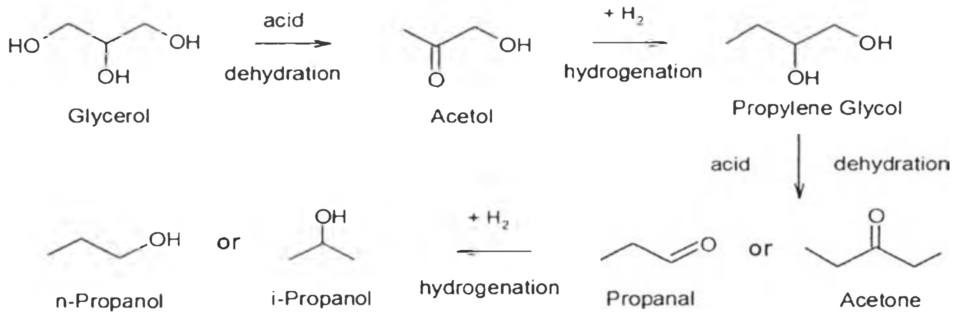

Figure 4.4 The glycerol conversion mechanism (Dasari *et al.*, 2005).

TPO profiles and percentages of carbon deposited on the spent catalysts as analyzed by temperature-programmed oxidation (TPO) are shown in Figure 4.5. It was found that the highest amount of coke was observed on the CuZnO/MgO (IWI) catalyst. This is probably due to the highest catalyst surface area. Coke deposition might poison the active site of the catalyst, which led to lower the catalytic activity. This result is in agreement with the loss in catalyst activities of the impregnated catalyst. This coke may be formed by unwanted polymerization of unsaturated intermediates, as reported by Ertl *et al.* (2008). Moreover, the coke obtained over the CuZnO/MgO (COP) catalyst can be removed at relatively lower temperature. In case of the CuZnO (COP), the lower amount of coke was observed comparing to the CuZnO/MgO (COP) catalyst. This could be because of the lower catalytic activity and catalyst surface area which led to the lower coke formation.

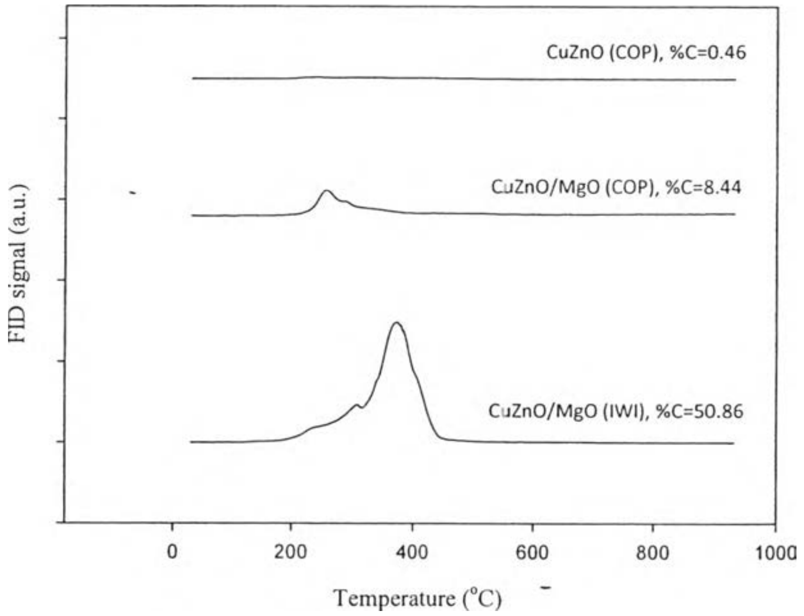

Figure 4.5 TPO profiles of the spent CuZnO/MgO catalysts with different preparation methods after 12 h TOS (Reaction conditions: 80 wt.% glycerol feed, 250 °C, 500 psig, H_2:glycerol = 4:1, and WHSV = 3.77 h^{-1}).

4.2.2 Effect of NaOH in Feedstock

Because of this present study is focused to use glycerol the by-product from biodiesel production, which is used KOH or NaOH as a catalyst. So, the glycerol may be consisted of these chemicals. Therefore, The effect of NaOH was investigated. The plot of glycerol conversion and propylene glycol selectivity as a function of time on stream over CuZnO/MgO catalysts on NaOH impurity in the glycerol feedstock—the refined glycerol, refined glycerol mixed with 0.1% NaOH is illustrated in Figure 4.6. The results showed that the refined glycerol mixed with 0.1% NaOH can be improved the glycerol conversion and propylene glycol selectivity in case of the CuZnO/MgO (COP) catalyst. This could because the addition of NaOH might enhance the performance of MgO in term of basicity, led to increase the conversion of glycerol and propylene glycol selectivity (Yuan *et al*,.2009) .Whereas, the glycerol conversion and propylene glycol selectivity of the CuZnO (COP) catalyst become decrease when adding small amount of NaOH in the glycerol feedstock, this might be due to Na poison the active site of catalyst. For the CuZnO/MgO (IWI) catalyst, the addition of 0.1% NaOH in the glycerol feedstock is not the significant factor for the glycerol conversion, but cause affect to reduce the propylene glycol selectivity. The increasing of catalytic activity might led the glycerol converted to other products—i.e. 2-propanol, and acetone that could reduce the propylene glycol selectivity (Dasari *et al*,.2005) whereas, the acetol and ethylene glycol selectivity did not completely change as shown in Figure 4.6 (c) and (d).

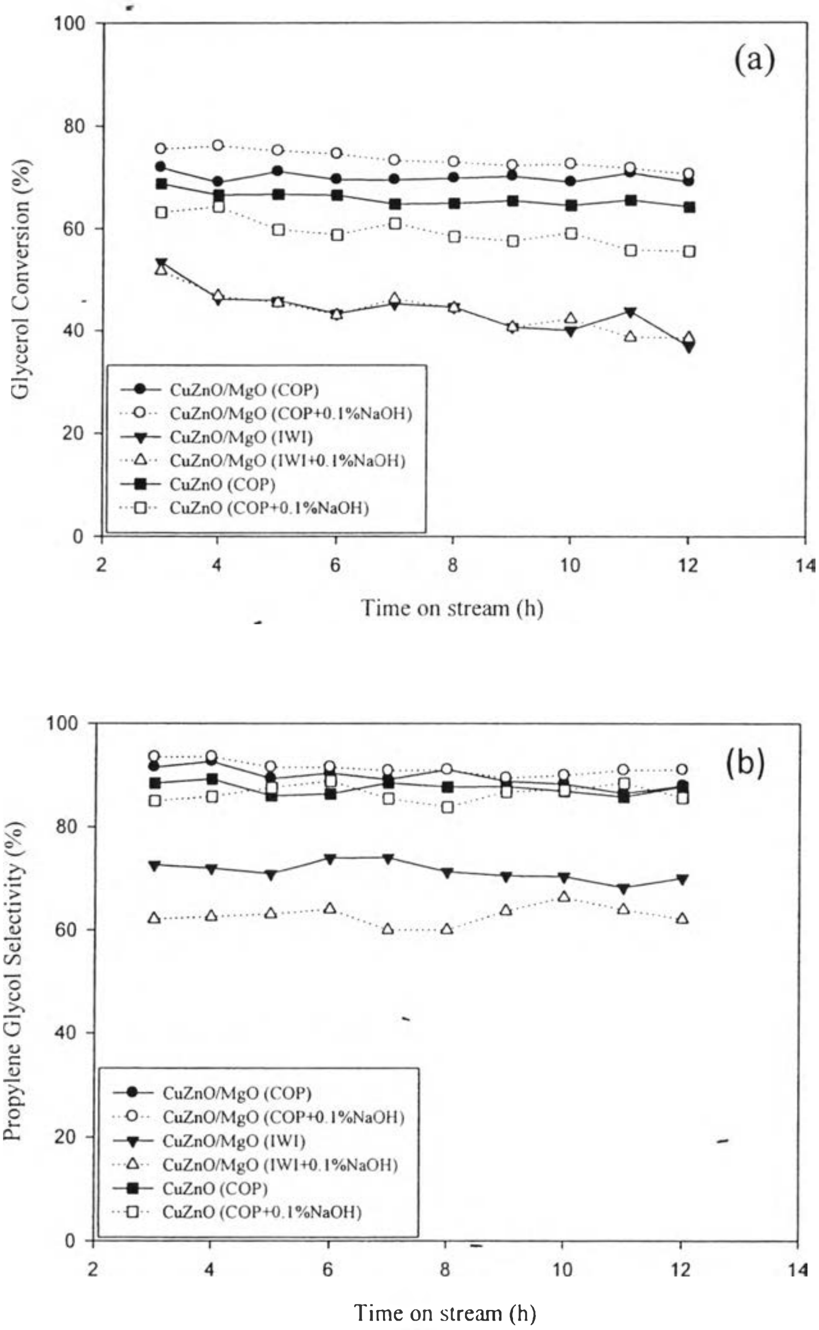

Figure 4.6 Plots of (a) Glycerol Conversion and (b) PG Selectivity (c) Acetol Selectivity (d) EG Selectivity as a function of time on stream over the CuZnO based catalysts prepared by different methods. (Reaction conditions: 80 wt.% glycerol feed, 250 °C, 500 psig, H_2:glycerol = 4:1, and WHSV = 3.77 h^{-1}).

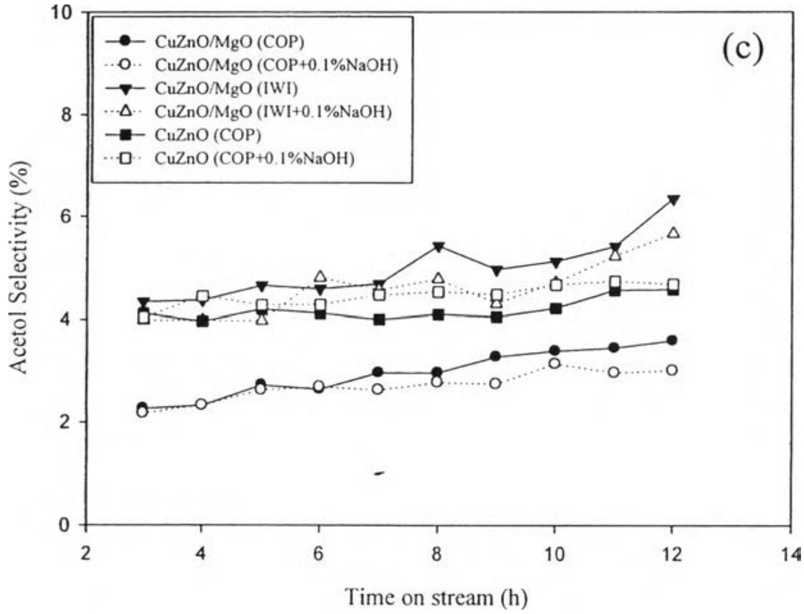

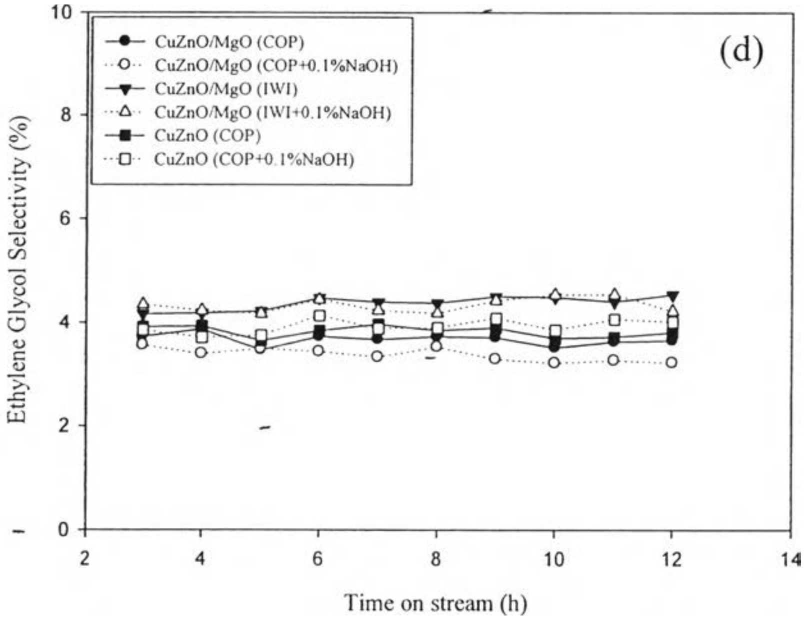

Figure 4.6 (cont.) Plots of (a) Glycerol Conversion and (b) PG Selectivity (c) Acetol Selectivity (d) EG Selectivity as a function of time on stream over the CuZnO based catalysts prepared by different methods. (Reaction conditions: 80 wt.% glycerol feed, 250 °C, 500 psig, H_2:glycerol = 4:1, and WHSV = 3.77 h^{-1}).

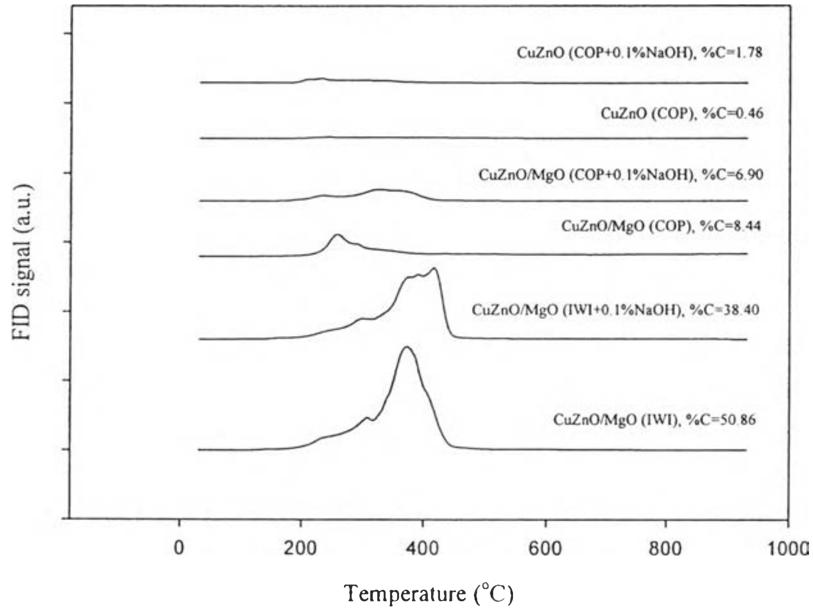

Figure 4.7 TPO profiles of CuZnO/MgO catalysts prepared by different methods on 0.1% NaOH impurities in the glycerol feedstock after 12 h TOS (Reaction conditions: 80 wt.% glycerol feed, 250 °C, 500 psig, H_2:glycerol = 4:1, and WHSV = 3.77 h^{-1}).

TPO profiles and the calculated amounts of carbon deposited on the spent catalysts on the effect of NaOH additional in the glycerol feedstock—the refined glycerol, the refined glycerol mixed with 0.1% NaOH is shown in Figure 4.7. The result showed that, the addition of NaOH in the glycerol feedstock can be reduced the coke deposition on the surface of CuZnO/MgO (IWI) and CuZnO/MgO (COP) catalysts. This could be because the higher pH value of the reaction solution on glycerol hydrogenolysis led to the more glycerol conversion and propylene glycol selectivity (Wang et al., 2007). Thus, the higher pH value might reduce the formation of coke.

Because of catalysts prepared by co-precipitation, CuZnO/MgO and CuZnO exhibited higher catalytic activity than that of prepared by impregnation, thus the co-precipitated catalysts was further characterized in order to study the effect of MgO consisting the catalyst. Figure 4.8 (a) exhibits Cu K-edge XANE spectra of the co-precipitated catalysts after the reduction and reference compounds. Cu foil shows an edge at 8981 eV and two characteristic peaks at the higher energy. Cu_2O and CuO possess different coordination and electronic structure, showing quite different spectra: the former shown an edge of Cu^+ at 8982 eV while, the letter oxide show an edge of Cu^{2+} at 8984 eV. Catalyst samples, CuZnO/MgO and CuZnO show the spectra quite similar to that of Cu foil, suggesting that the Cu species basically exists as Cu metal form in the catalysts. However, the edges spectra of catalyst samples were similar. The Zn K-edge spectra, ZnO shows an edge at 9663 eV and two peaks at 9669 and 9680 eV (Figure 4.8 (b)). No significant change was observed in the spectra between the CuZnO/MgO catalysts and ZnO. For the CuZnO catalyst, the observed peak apparently indicates the presence of a Zn species different from bulk ZnO.

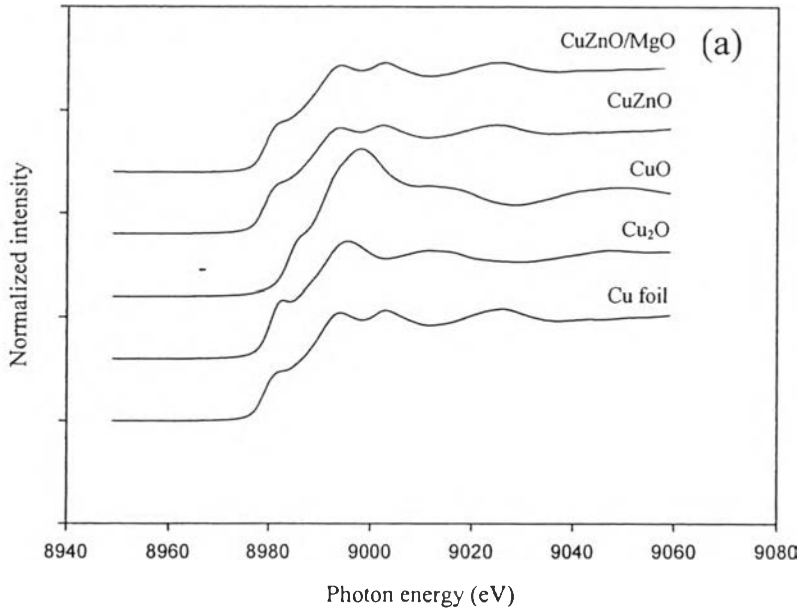

Figure 4.8 Cu (a) and Zn (b) K-edge XANES spectra of the co-precipitated CuZnO/MgO, CuZnO catalysts and reference compounds.

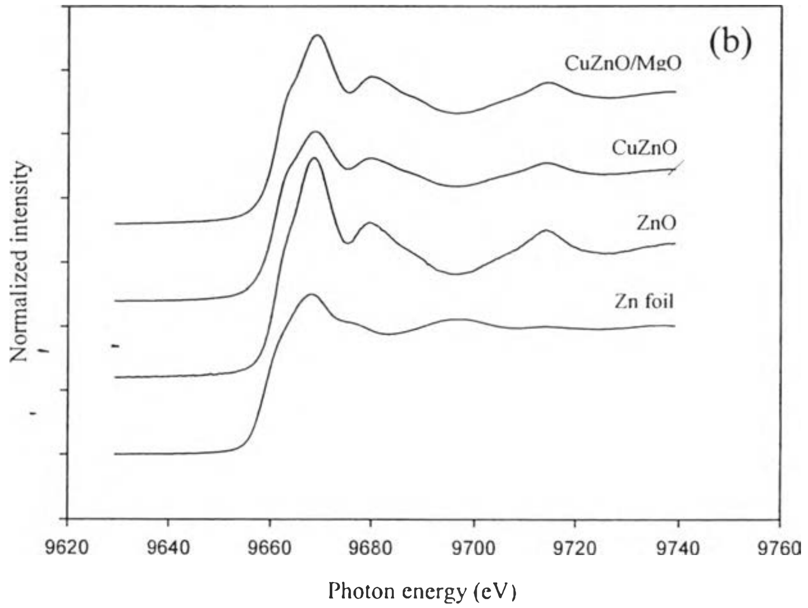

Figure 4.8 (cont.) Cu (a) and Zn (b) K-edge XANES spectra of the co-precipitated CuZnO/MgO, CuZnO catalysts and reference compounds.

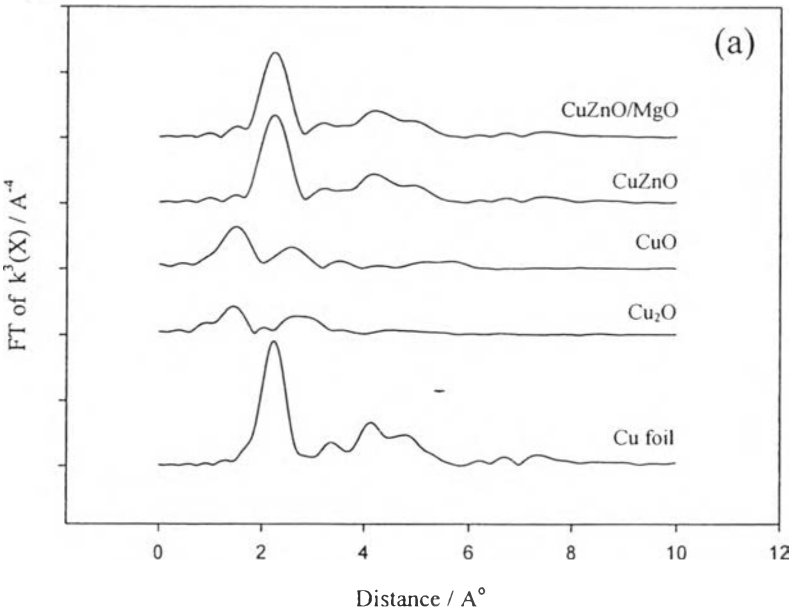

Figure 4.9 Fourier transform of k^3-weighed Cu (a) and Zn (b) K-edge EXAFS spectra of the co-precipitated CuZnO/MgO, CuZnO catalysts and reference compounds.

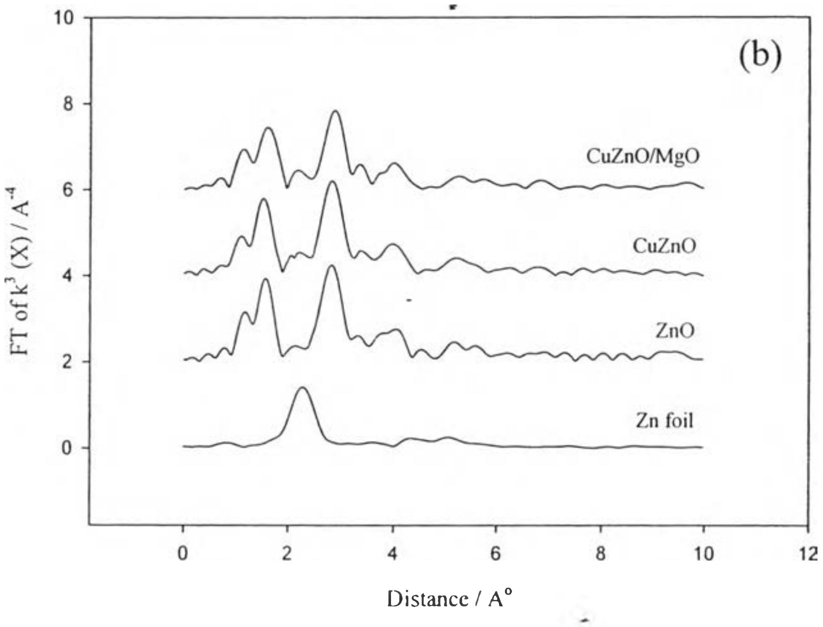

Figure 4.9 (cont.) Fourier transform of k^3-weighed Cu (a) and Zn (b) K-edge EXAFS spectra of the co-precipitated CuZnO/MgO, CuZnO catalysts and reference compounds.

Cu K-edge EXAFS spectra of the co-precipitated catalysts after the reduction and reference compounds are shown in Figure 4.9 (a). The spectra were almost similar for both catalyst samples CuZnO/MgO and CuZnO. Peaks were observed at 2.2 A°, represented the Cu metal form in the catalyst that independenly on Mg content. Zn-edge spectra (Figure 4.9 (b)) were also investigated for two catalyst samples. The CuZnO/MgO catalyst showed peak at 1.5 and 3 A°, coinciding with the bond distance of Zn–O and Zn–Zn in ZnO independently on the MgO content. However, the CuZnO catalyst showed the peak different from the peak of CuZnO/MgO and ZnO. Two shoulder peaks were observed around 2.1 A° that represent the characteristic peak of Cu foil and Zn foil respectively. This result indicates the presence of Cu–Zn alloy in the CuZnO catalyst. The presence of alloy species leads to lose of some Cu active sites, as well agreed with the model proposed by Grunwaldt *et al.* (2000) (Figure 4.10).

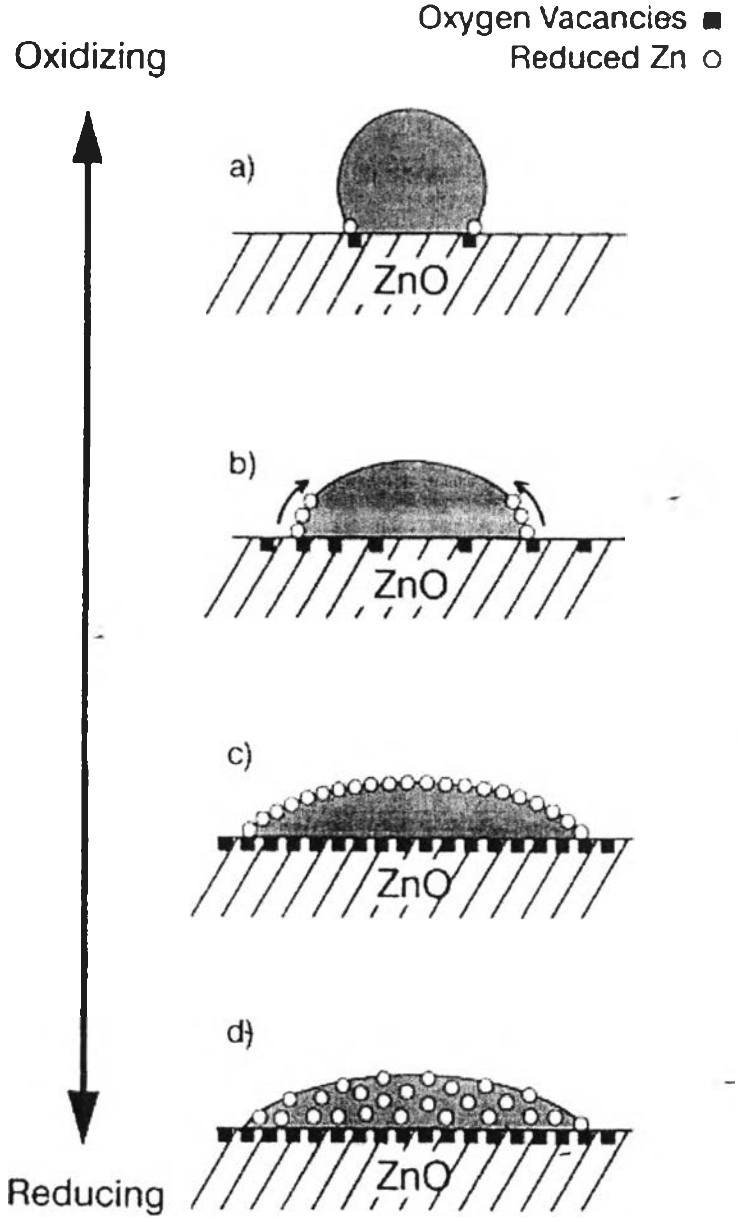

Figure 4.10 Schematic model for the Cu particles on Zn support, surface alloying, and bulk alloy formation: (a) under oxidation conditions (b) under more reducing conditions (c) strong reducing conditions (d) severe reducing conditions (Grunwaldt *et al.*, 2000).

4.3 Catalytic Stability Testing and Catalyst Regeneration

Noticeably, The CuZnO/MgO catalyst prepared by COP exhibited the highest catalytic activity. Thus, this catalyst was selected to study for its stability and the spent of the co-precipitated was regenerated in-situ at 490 °C for 3 h in order to eradicate deposited carbon on the surface of catalyst. After calcinations and reduction, the regenerated catalyst was tested for its activity in the same condition as the fresh catalyst.

4.3.1 Catalytic Stability Testing

The catalytic stability testing of the co-precipitated catalyst was tested for 39 h of time on stream. The glycerol conversion and propylene glycol selectivity were tested for comparing between pure feedstock and NaOH additional in the glycerol feedstock as shown in figure 4.10. The experimental results demonstrated that the glycerol conversion of the catalyst with pure feedstock still remain stable around 70 % until 27 h of reaction. After, the glycerol conversion become rapidly decrease to 20 % at 39 h of reaction. For the effect of NaOH additional in the glycerol feedstock, the result showed that the glycerol conversion remain stable around 75 % for 12 h of reaction and after, the glycerol conversion slightly decrease to 45 % at 39 h of reaction. This result could be because the addition of NaOH not only performs the activity for the catalyst but it also act like a coke retarder. Thus, the glycerol conversion was not rapidly decrease compared to the pure glycerol feedstock. The result is well agreed with the TPO result as mentioned in **4.4.2** . However, the propylene glycol selectivity remains stable until 39 h of time on stream both of in the pure glycerol feedstock and the NaOH additional in the glycerol feedstock.

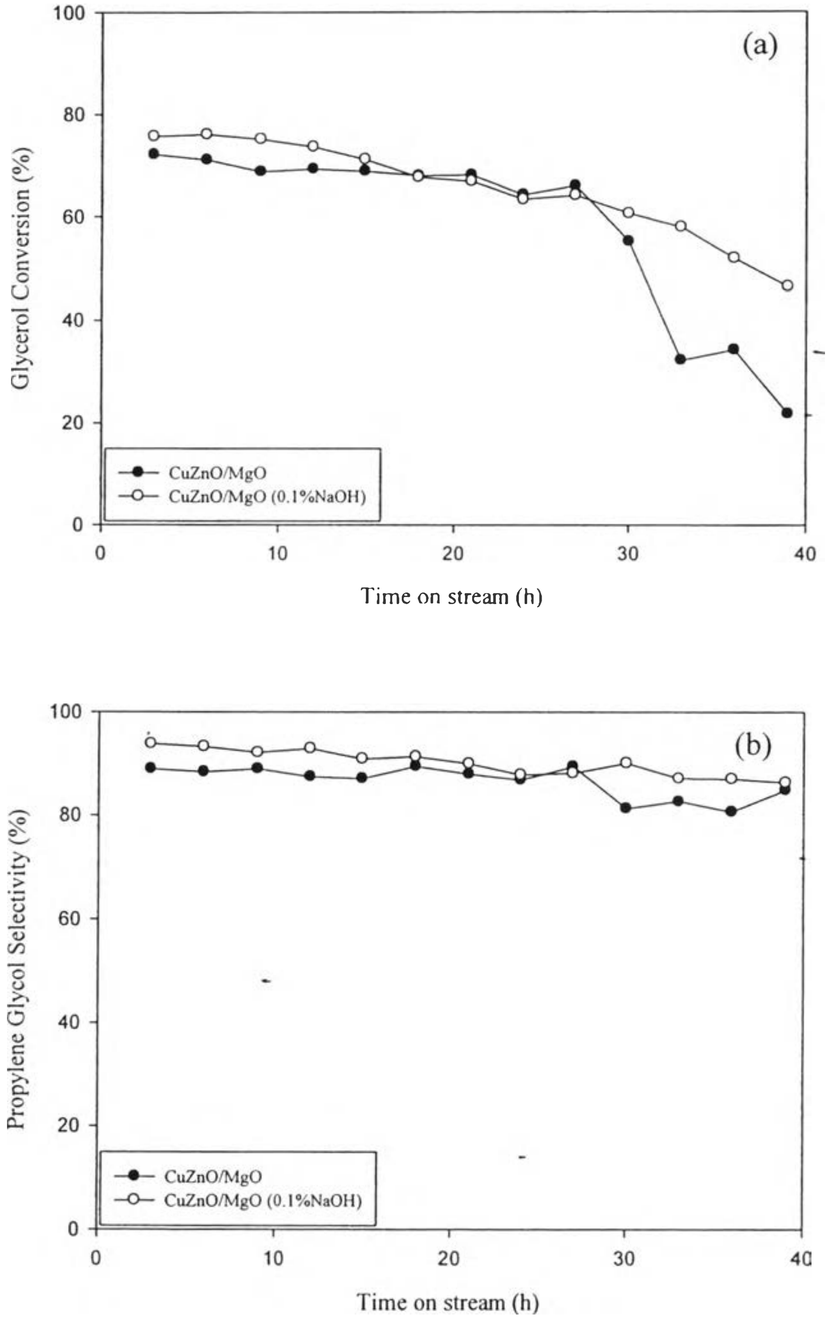

Figure 4.11 Plots of (a) Glycerol Conversion and (b) PG Selectivity as a function of time on stream over the CuZnO/MgO catalysts prepared by co-precipitation methods. (Reaction conditions: 80 wt.% glycerol feed, 250 °C, 500 psig, H_2:glycerol = 4:1, and WHSV = 3.77 h^{-1}).

4.3.2 Catalyst Regeneration

Figure 4.11 demonstrated that, the glycerol conversion of the regenerated catalyst was as good as fresh catalyst. Moreover the propylene glycol selectivity (Figure 4.11) was lower than that of the fresh catalyst which the constant of ethylene glycol selectivity and the increase of acetol selectivity, as shown in Figure 4.11(c) and (d) respectively, this could be because the agglomeration of CuO particles.

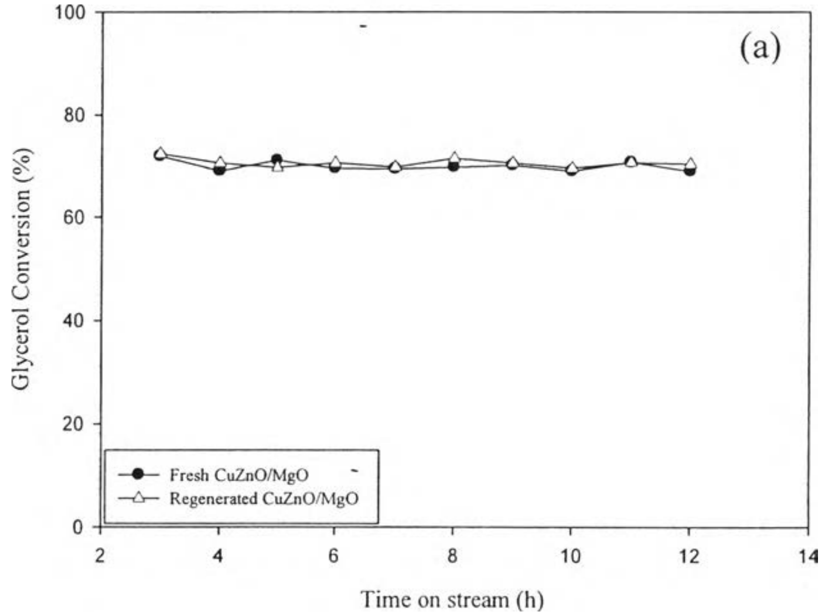

Figure 4.12 Plots of (a) Glycerol Conversion and (b) PG Selectivity (c) Acetol Selectivity (b) EG Selectivity as a function of time on stream over the CuZnO/MgO catalysts prepared by co-precipitation methods. (Reaction conditions: 80 wt.% glycerol feed, 250 °C, 500 psig, H_2:glycerol = 4:1, and WHSV = 3.77 h^{-1}).

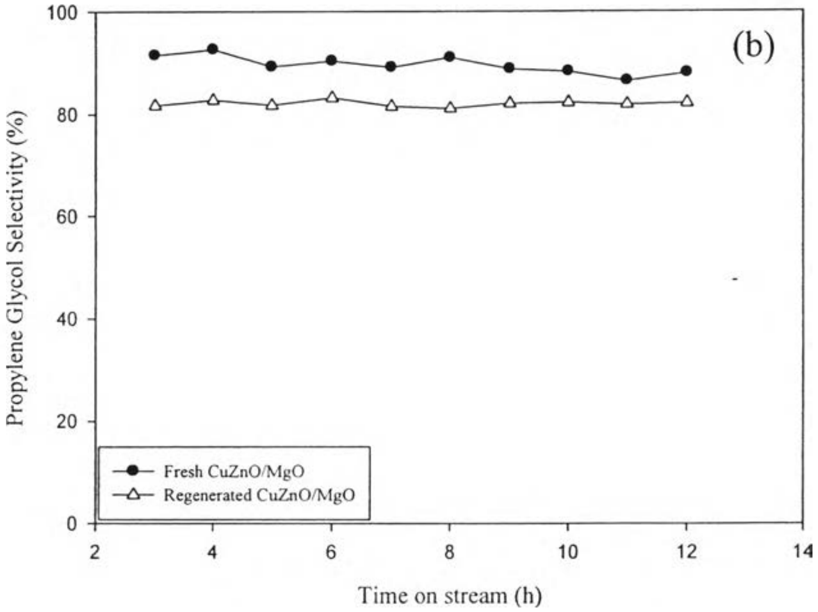

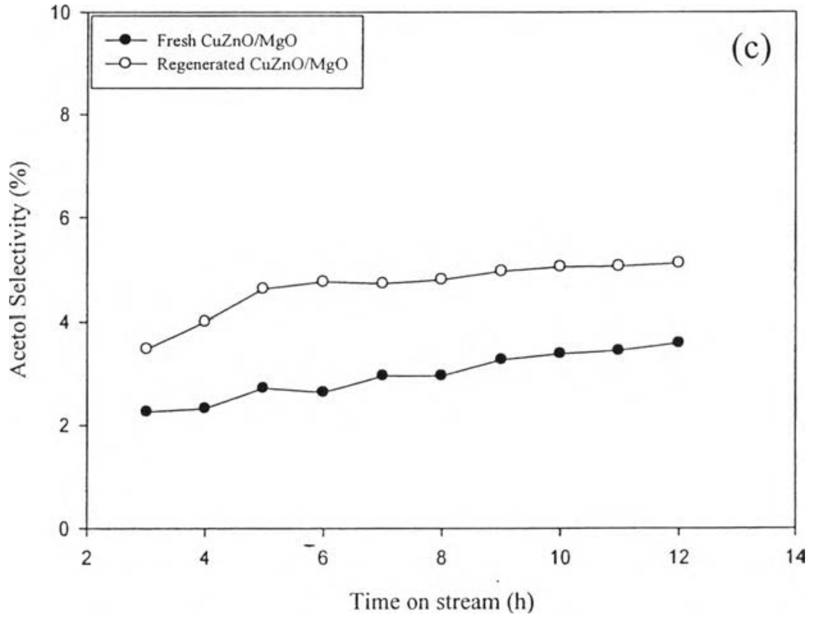

Figure 4.12 (cont.) Plots of (a) Glycerol Conversion and (b) PG Selectivity (c) Acetol Selectivity (b) EG Selectivity as a function of time on stream over the CuZnO/MgO catalysts prepared by co-precipitation methods. (Reaction conditions: 80 wt.% glycerol feed, 250 °C, 500 psig, H_2:glycerol = 4:1, and WHSV = 3.77 h^{-1}).

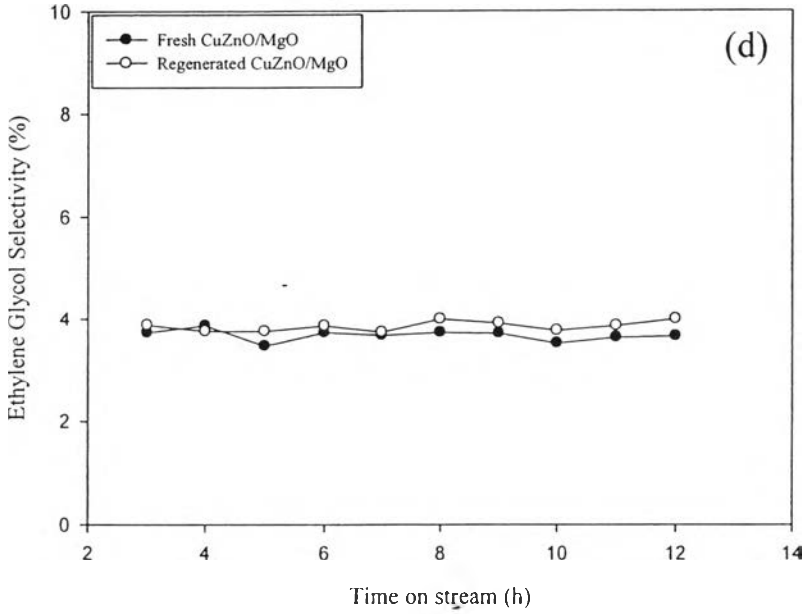

Figure 4.12 (cont.) Plots of (a) Glycerol Conversion and (b) PG Selectivity (c) Acetol Selectivity (b) EG Selectivity as a function of time on stream over the CuZnO/MgO catalysts prepared by co-precipitation methods. (Reaction conditions: 80 wt.% glycerol feed, 250 °C, 500 psig, H_2:glycerol = 4:1, and WHSV = 3.77 h^{-1}).

The effect of NaOH additional in the glycerol feedstock, Figure 4.12 (a) and (b) shows the conversion and propylene glycol selectivity. Results show that, the glycerol conversion was remaining as ever. However, the propylene glycol selectivity becomes lower than that of the fresh catalyst moreover, it was more decrease compared to the pure glycerol feedstock which the increase of acetol and ethylene glycol selectivity, as shown in Figure 4.12 (c) and (d) this is probably due to the agglomeration of CuO particles and Na deposited in the active site of the catalyst, as referred by AAS in Table 4.3. The concentration of 4.45 ppm Na metal was detected in the spent catalyst after the first run and show higher concentration of Na metal in the spent catalyst after the second run.

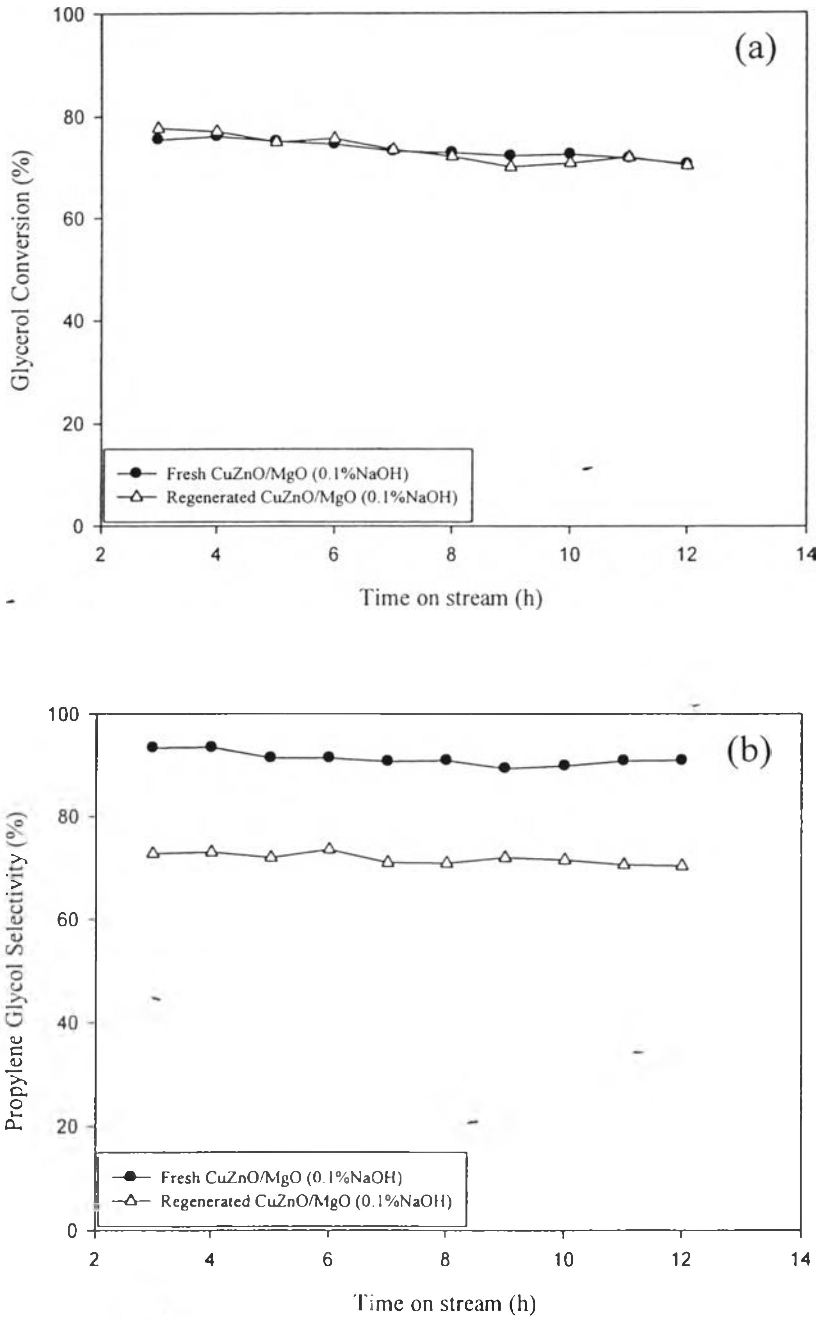

Figure 4.13 Plots of (a) Glycerol Conversion and (b) PG Selectivity (b) Acetol Selectivity (b) EG Selectivity as a function of time on stream over the CuZnO/MgO catalysts prepared by co-precipitation methods. (Reaction conditions: 80 wt.% glycerol feed, 250 °C, 500 psig, H_2:glycerol = 4:1, and WHSV = 3.77 h^{-1}).

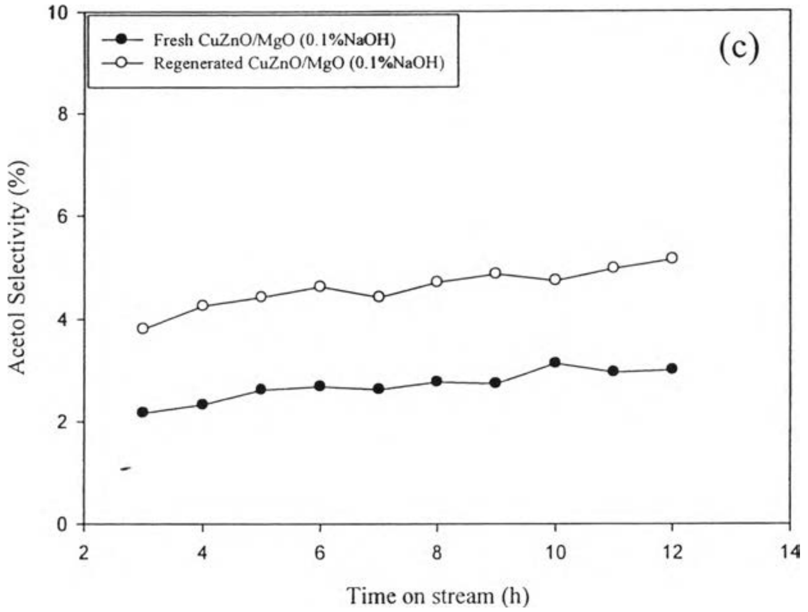

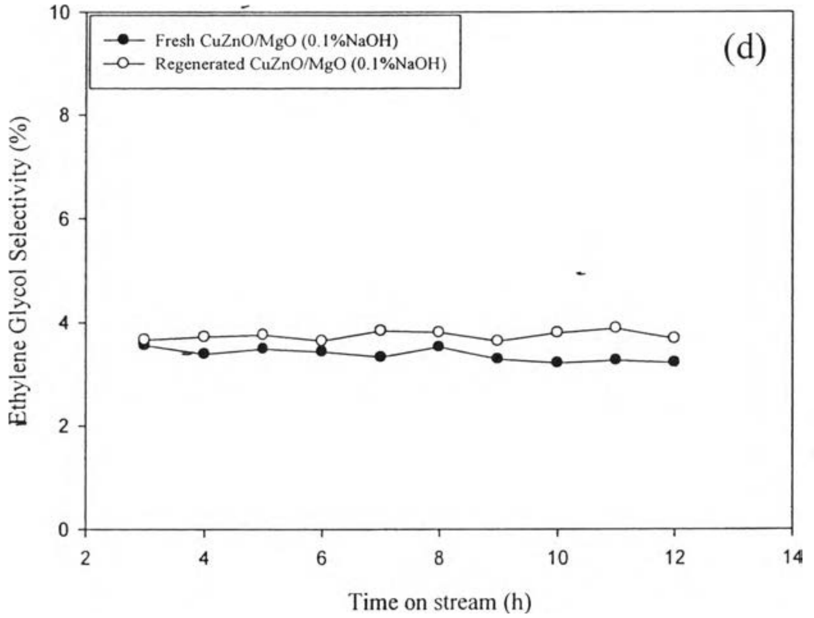

Figure 4.13 (cont.) Plots of (a) Glycerol Conversion and (b) PG Selectivity (b) Acetol Selectivity (b) EG Selectivity as a function of time on stream over the CuZnO/MgO catalysts prepared by co-precipitation methods. (Reaction conditions: 80 wt.% glycerol feed, 250 °C, 500 psig, H_2:glycerol = 4:1, and WHSV = 3.77 h^{-1}).

Table 4.3 Concentration of alkali on feedstock, product, and the spent co-precipitated CuZnO/MgO catalysts analyzed by AAS

Catalyst	**Feedstock (ppm)**	**Product (ppm)**	**Spent catalyst after 1st run (ppm)**	**Spent catalyst after 2nd run (ppm)**
CuZnO/MgO	897.00	749.00	4.45	6.38

Figure 4.13 (a) and (b) demonstrated that the carbon deposited on the regenerated catalyst compared to the fresh catalyst in pure glycerol feedstock and NaOH containing glycerol feedstock respectively. The result showed that, the regenerated catalyst exhibited a less carbon deposit than that of the fresh catalyst; this might be due to the loss of some active sites in the catalyst during the first run and led to less reaction and coke formation. Figure 4.14 exhibited the XRD patterns of the fresh and regenerated CuZnO/MgO catalysts. The results showed that each species (CuO, ZnO) of regenerated catalyst both in pure glycerol feedstock and NaOH containing glycerol feedstock show the peak patterns at the same position as the fresh catalyst. This result indicated that, the regeneration process did not affect the crystalline phases of catalysts.

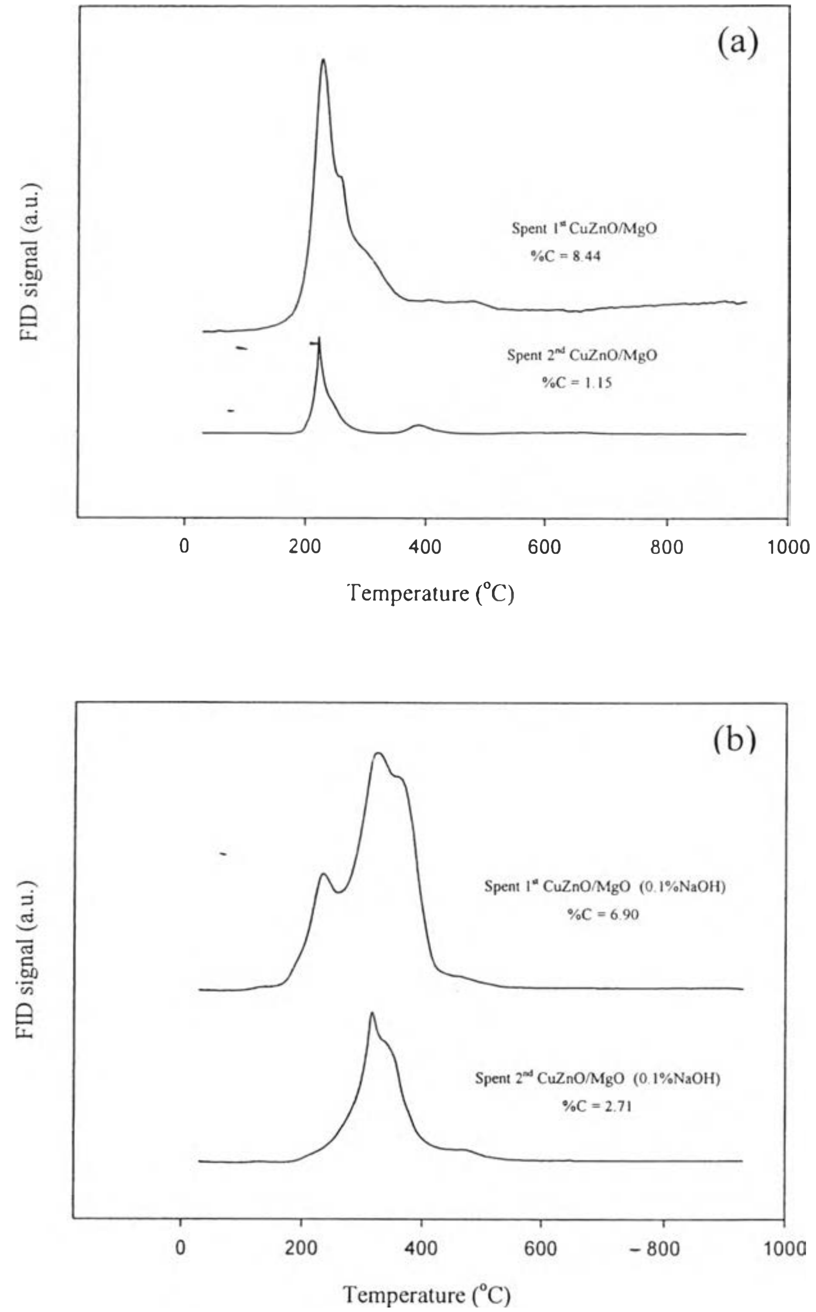

Figure 4.14 TPO profiles of the spent CuZnO/MgO catalysts after 12 h TOS (a) pure glycerol feedstock (b) 0.1% NaOH containing glycerol feedstock.

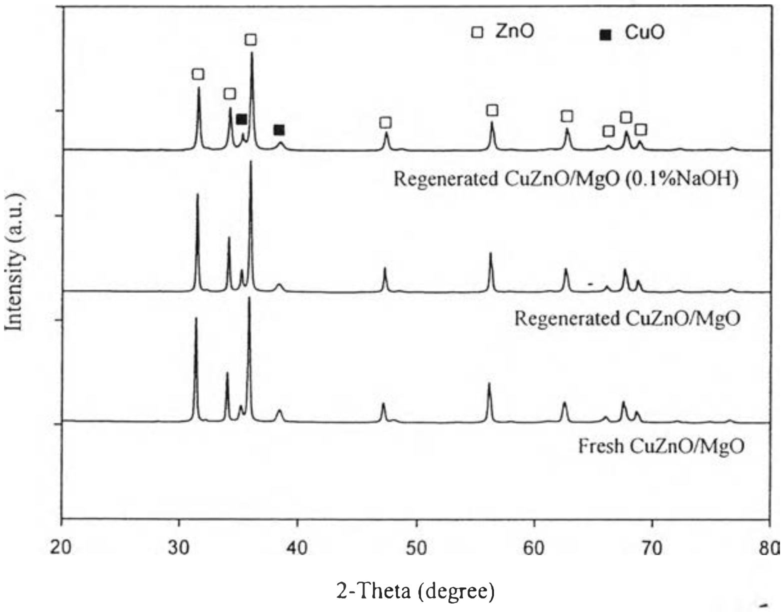

Figure 4.15 XRD patterns of the fresh and regenerate co-precipitated CuZnO/MgO catalysts after 12 h TOS.

The H_2–TPR profiles of the fresh and regenerated catalyst are shown in Figure 4.15. The reduction peak of the regenerated catalyst both of pure glycerol feedstock and NaOH additional in the glycerol feedstock shifted to higher temperature compared to the fresh catalyst. This result indicated that, the CuO particles would aggregate to form the larger grains of particles after cause of reaction. The H_2–TPR profiles of the fresh and regenerated catalysts with NaOH additional in glycerol feedstock consisting of the main peak and small shoulder peak were observed, a main peak at 290 °C and a small shoulder at 250 °C was observed in the former, whereas the latter, a main peak was observed at 300 °C and at 270 °C for a small shoulder. The H_2–TPR profile of regenerated catalyst with pure glycerol feedstock show a main single peak at 310 °C, this peak represented the reduction of large grains of CuO particles.

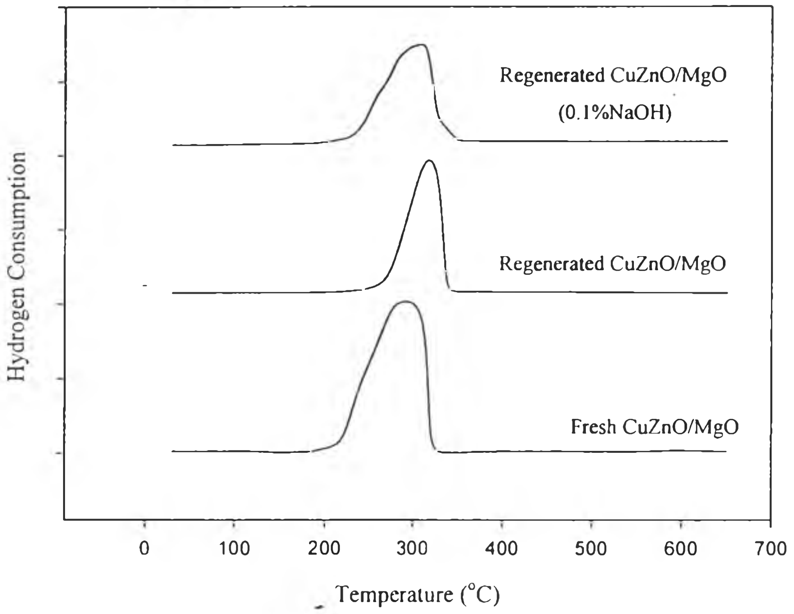

Figure 4.16 Temperature programmed reduction (TPR) profiles of the fresh and regenerate co-precipitated CuZnO/MgO catalysts.